

New Catalysts for Hydroprocessing: Bimetallic Oxynitrides

II. Reactivity Studies

Sasangan Ramanathan, C. Charles Yu, and S. Ted Oyama¹

Laboratory for Environmental Catalysis and Materials, Department of Chemical Engineering, Virginia Tech, Blacksburg, Virginia 24061-0211

Received August 13, 1996; revised June 24, 1997; accepted September 3, 1997

Bimetallic oxynitrides of the type $M_1M_2O_xN_y$ were used as catalysts in hydrotreating reactions at 3.1 MPa and 643 K. The catalysts were prepared by nitriding bimetallic oxide precursors, where MoO_3 or WO_3 was one of the components, as described in the companion paper. The reactions were studied in a three-phase trickle-bed reactor operated at 3.1 MPa and 643 K. The feed was a model liquid mixture containing 3000 ppm sulfur (dibenzothiophene), 2000 ppm nitrogen (quinoline), 500 ppm oxygen (benzofuran), 20 wt% aromatics (tetralin), and balance aliphatics (tetradecane). The activities of the bimetallic nitrides were compared to a commercial sulfided Ni-Mo/ Al_2O_3 catalyst tested at the same conditions. The bimetallic oxynitrides were active for HDN of quinoline with V-Mo-O-N showing higher HDN activity than the commercial sulfided Ni-Mo-S/ Al_2O_3 catalyst. The HDS activity of the bimetallic oxynitrides ranged from 9 to 37% with Co-Mo-O-N showing the highest HDS activity among the oxynitrides tested. X-ray diffraction analysis of the spent catalysts indicated that the oxynitrides consisting of early transition metals (Group 4–Group 6) were tolerant of sulfur, while catalysts involving metals of Group 7 and Group 8 showed bulk sulfide phases. X-ray photoelectron spectroscopic analysis of the catalysts before and after the reaction indicated the incorporation of sulfur on the surface of the catalysts after prolonged exposure to the reactants. © 1998 Academic Press

transfer reactions (3) and considerable attention has been placed on hydroprocessing applications. Schlatter *et al.* (4) and Sajkowski and Oyama (5) carried out the first comprehensive comparison of different compounds and showed that Mo_2N and Mo_2C had good activity in the HDN of quinoline. Recent studies have confirmed this initial report, showing that Mo_2N was indeed active in the HDN of quinoline (6) as well as pyridine (7), indole (8), and carbazole (9) and that the catalyst was stable under prolonged exposure to sulfur at higher temperature (10). A comparative study of simultaneous quinoline HDN and thiophene HDS in the gas phase showed the activity to follow the order $Mo_2N > W_2N > VN/SiO_2 > TiN$ (11). A recent comprehensive study (12) repeats the comparison of a series of monometallic carbides and nitrides of optimized surface area prepared by temperature programmed reaction. Activity for quinoline HDN follows the order Group 6 > Group 5 > Group 4 with Mo_2C showing higher HDN activity than a commercial sulfided Ni-Mo-S/ Al_2O_3 (shell 324). In an attempt to improve the HDN activity and the stability of monometallic nitrides, we prepared a new class of catalysts for HDN consisting of bimetallic oxynitrides and tested them for activity in hydroprocessing.

INTRODUCTION

Catalytic hydroprocessing to remove heteroatoms like sulfur, nitrogen, and oxygen from petroleum feedstocks is a critical step in the refining of hydrocarbon resources. It is known that hydrodenitrogenation (HDN) is more difficult than hydrodesulfurization (HDS), since C–N bonds are stronger than C–S bonds, and nitrogen removal requires prior ring saturation (1). Conventional hydrotreating catalysts are found to be active for HDN, but the demand for denitrogenation-selective catalysts will grow with the need to process heavier resources, and possibly, synthetic feedstocks derived from coal (2).

Transition metal carbides and nitrides have been reported to exhibit catalytic activity in a number of hydrogen-

EXPERIMENTAL

Materials

Chemicals used in this study were tetradecane (Jansen Chimica, 99.5%), quinoline (Aldrich, 99.5%), benzofuran (Aldrich, 99.5%), tetralin (Aldrich, 99.5%), and dibenzothiophene (Aldrich, 99%). The gases employed were H_2 (Airco Grade 5, 99.999%), 10% H_2S/H_2 (Airco Grade 5, 99.999%), He (Airco Grade 5, 99.999%) and air (Airco Grade dry, 99.99%).

Catalytic Testing

Catalysts were tested in a three-phase trickle-bed reactor described in a previous publication (12). The reactors were 19 mm/16 mm OD/ID 316 SS tubes with a central thermocouple to measure the temperature of the catalyst bed.

¹ To whom correspondence should be addressed.

Hydrogen flow to the reactors was regulated by mass flow controllers (Brooks, model 5850E) and liquid was metered from burettes by high-pressure liquid pumps (LDC Analytical, model NCI-1105). Liquid samples were collected downstream in sealed septum vials and analyzed off-line by gas chromatography.

The bimetallic oxynitrides were tested for their activity in hydrogenation (HYD), hydrodenitrogenation (HDN), hydrodesulfurization (HDS), and hydrodeoxygenation (HDO) using model liquid compounds at 643 K and 3.1 MPa. HYD refers to hydrogenation of aromatic rings without removal of hetero-atoms, whereas HDN, HDS, and HDO refer to the total removal of N, S, and O respectively. Hence, for example, the percent HDN refers to the percent of quinoline converted to products free of nitrogen. The liquid feed mixture used in all the experiments consisted of 3000 ppm sulfur (dibenzothiophene), 2000 ppm nitrogen (quinoline), 500 ppm oxygen (benzofuran), 20 wt% aromatics (tetralin), and balance aliphatics (tetradecane). A typical experiment consisted of loading about 0.2–1 g of catalyst (powder of particle size ca. 1 μm), equivalent to a total surface area of 30 m^2 . The powders were diluted to a constant bed volume of 1 cm^3 with quartz chips (16/20 mesh). A 10% $\text{H}_2\text{S}/\text{H}_2$ gas mixture was used to sulfide the commercial Ni–Mo/ Al_2O_3 catalyst while pure H_2 was used to activate the bimetallic oxynitrides. The pretreatment was carried out *in situ* at 723 K and atmospheric pressure for 3 h. The reactors were cooled down to the reaction temperature (643 K) and hydrogen was pressurized to 3.1 MPa. A liquid feed rate of 5 $\text{cm}^3 \text{h}^{-1}$ and a hydrogen flow rate of 150 $\text{cm}^3(\text{NTP})/\text{min}$ (100 $\mu\text{mol s}^{-1}$) were used in all the reactions. Space velocity was calculated using the apparent catalyst bed volume. Liquid samples were collected at regular intervals for about 60 h by which time the catalysts showed steady state activity.

After the reaction the catalysts were extracted with hexane solvent for about 24 h to wash out any residual feed liquid off the surface and were air dried until the solvent evaporated. The bulk phase purity of the spent catalysts was checked by X-ray diffraction (XRD) using a powder diffractometer (Siemens, model D500 with Cu $K\alpha$ monochromatized radiation source) operated at 40 kV and 30 mA. The changes in the surface composition of the catalysts were obtained by X-ray photoelectron spectroscopy (XPS) (Perkin Elmer, model 5300 with Mg source) operated at 15 kV and 30 mA. C 1s (285.0 eV) was used as reference in the analysis and the atomic concentration of the individual elements was calculated from the peak area and atomic sensitivity factor (13).

RESULTS AND DISCUSSION

The activities of the oxynitrides and the commercial Ni–Mo catalyst were compared on an equal reactor loaded

TABLE 1
Summary of Catalyst Performance in Hydroprocessing at 3.1 MPa and 643 K: LHSV = 5 h^{-1}

Catalyst	QNL conv.% HYD + HDN	HDN %	HDS %	HDO %	Spacetime $10^3/\text{cm}^3 \text{g}^{-1} \text{s}^{-1}$
Quartz chips	48	0	4	2	0.7
NiMo/ Al_2O_3	85	38	79	63	3.8
V–Mo–O–N	89	44	25	32	1.8
Mo–W–O–N	74	34	18	16	5.6
Cr–Mo–O–N	72	31	15	12	4.1
Nb–Mo–O–N	74	27	9	31	5.6
Co–W–O–N	73	24	35	16	2.0
Co–Mo–O–N	63	22	37	16	5.4
Mn–Mo–O–N	65	21	24	—	1.7
V–W–O–N	49	1	1	6	2.8

surface area of 30 m^2 . Comparison on this basis may seem to favor the unsupported oxynitrides over the supported Ni–Mo catalyst; however, the commercial catalyst is of high loading (>20 wt%) and is highly optimized, and most of its surface area should be active. Hence, a comparison based on equal surface areas should give a good approximation of the relative activities of the catalysts. The performance of bimetallic oxynitrides in hydroprocessing at 3.1 MPa and 643 K with moderate concentrations of N, S, O, and aromatics is summarized in Table 1. HYD refers to hydrogenation of quinoline to N-containing compounds. Bimetallic oxynitrides with Mo as one of the metals were found to be active for quinoline HDN. The HDN activity of the oxynitrides ranged from 21–44% with V–Mo–O–N showing higher HDN activity than the commercial Ni–Mo–S/ Al_2O_3 catalyst. The hydrodesulfurization activity of the oxynitrides ranged from 9 to 37% and the hydrodeoxygenation (HDO) activity ranged from 6 to 32%. V–W–O–N was found to be inactive for all the reactions studied, while Co–W–O–N showed considerable HDS and HDN activities. In fact, both molybdenum and tungsten when alloyed with cobalt exhibited higher catalytic activity. The performance of monometallic nitrides under the same

TABLE 2
Activity of Monometallic Nitrides in HDN, HDS, and HDO at 3.1 MPa and 643 K

Catalyst	% Quinoline conversion	%HDN	%HDS	%HDO
Mo_2N	73	23	16	10
WO_xN_y^a	60	20	5	11
NbO_xN_y^b	27	13	—	—
VN	66	5	3	43
TiN	43	3	3	4

^a Reference (24).

^b Reference (25).

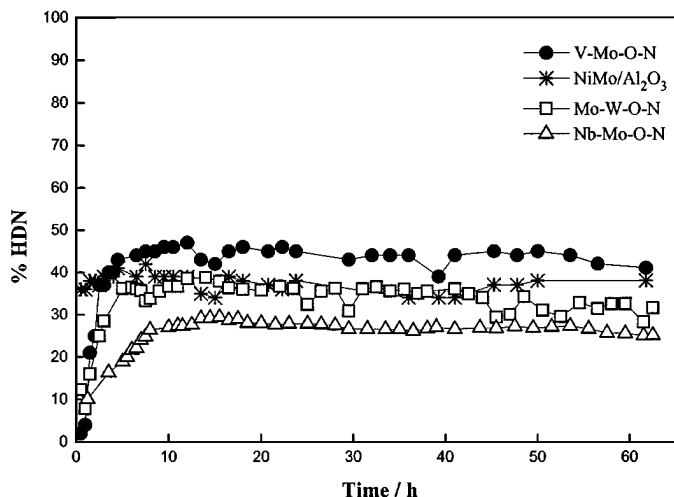


FIG. 1. Comparison of HDN activities of Ni-Mo/Al₂O₃, V-Mo-O-N, Mo-W-O-N, and Nb-Mo-O-N at 3.1 MPa and 643 K.

conditions is given in Table 2. These compounds showed HDN conversions in the range 5–23% with the order of activity being Mo₂N > W₂N > VN > TiN, i.e., Group 6 > Group 5 > Group 4. The HDN activity is seen to be lower than the bimetallic compounds.

Figure 1 shows a comparison of the steady state HDN activities of the oxynitrides with the commercial Ni-Mo-S/Al₂O₃ catalyst, and for clarity only the active catalysts are presented. The HDN activity of the oxynitrides with Mo as one of the components followed the order V-Mo > Mo-W > Cr-Mo > Nb-Mo > Co-W > Co-Mo > Mn-Mo > V-W. The relative activities of the catalysts are probably due to the differences in the ease of reducibility of the catalysts during the activation process. As shown in the companion paper (Fig. 3) the compounds could be divided into three groups according to their reducibility (high, medium, low) and followed the order V-Mo > Cr-Mo > Co-Mo > Mo-W > Co-W > Mn-Mo > V-W > Nb-Mo. Easily reduced compounds, V-Mo, Cr-Mo, and Co-Mo, showed two features in water formation at around 595 and 738 K. Compounds less easily reduced, Mo-W, Co-W, and Mn-Mo, showed a single high-temperature broad feature at 738 K. The compounds least easily reduced, Nb-Mo and V-W, had narrow reduction features appearing at the highest temperatures. The order in reducibility, with minor deviation, follows closely the order in reactivity. The lower HDN activity of Co-Mo compared to V-Mo and Cr-Mo is not surprising because of the formation of bulk sulfide, as will be discussed later. In fact, compounds with the late transition elements (Co-Mo, Co-W, Mn-Mo) showed a propensity to form sulfides and to have low activity. Mo-W and Nb-Mo showed higher HDN activity than was expected possibly due to the better sulfur tolerance of these catalysts. Finally V-W had low activity, despite tolerance to sulfur, because of an inherent low activity

of its component elements. VN and W₂N have very poor reactivity in HDN (11, 14).

Figure 2 shows a comparison of the steady state HDS activities of the catalysts at 643 K and 3.1 MPa. For clarity, Ni-Mo/Al₂O₃, V-Mo-O-N, Mo-W-O-N, and Nb-Mo-O-N are presented in the figure. The HDS activity of the oxynitrides followed the order Co-Mo > Co-W > V-Mo > Mn-Mo > Mo-W > Cr-Mo > Nb-Mo > V-W, which did not track reducibility. Instead the trend here appears to follow the position in the periodic table of the secondary (non-Mo or W) alloying element (Group 8 > Group 7 > Group 6 > Group 5). This implies that HDS and HDN occur on different sites. The higher HDS activity of the cobalt-containing catalysts was due to the formation of bulk cobalt sulfide (Co₄S₃), while all other samples show high initial activities, but significant deactivation over the course of the first 30–40 h. The HDS activity of the Co-containing oxynitrides is concurrent with earlier reports (15, 16) which showed that among the first-row transition metal sulfides a maximum in the HDS activity was observed for Group 9 (Co) and Group 10 (Ni). In addition, the heat of formation of cobalt sulfide is intermediate in nature compared to the higher values of chromium, molybdenum, and tungsten sulfides (15). The higher HDS activity of Co-Mo and Co-W catalysts could be due to the optimum binding energy of the sulfur-containing molecule on the Co₄S₃ surface compared to the rest of the catalysts which indicated a partial surface sulfide (XPS data presented later). The sulfided Ni-Mo-S/Al₂O₃ catalyst showed a short induction period and a sustained high level of desulfurization with better HDS activity than the bimetallic oxynitride catalysts. Biphenyl was the only product detected from HDS of dibenzothiophene and no further hydrogenation of biphenyl was observed.

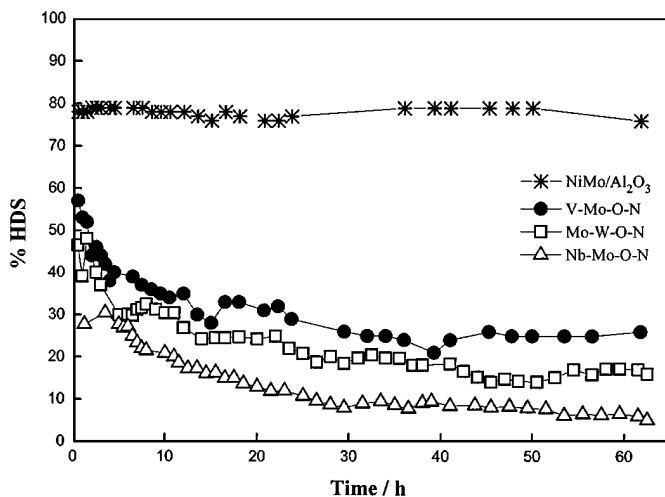


FIG. 2. Comparison of HDS activities of Ni-Mo/Al₂O₃, V-Mo-O-N, Mo-W-O-N, and Nb-Mo-O-N at 3.1 MPa and 643 K.

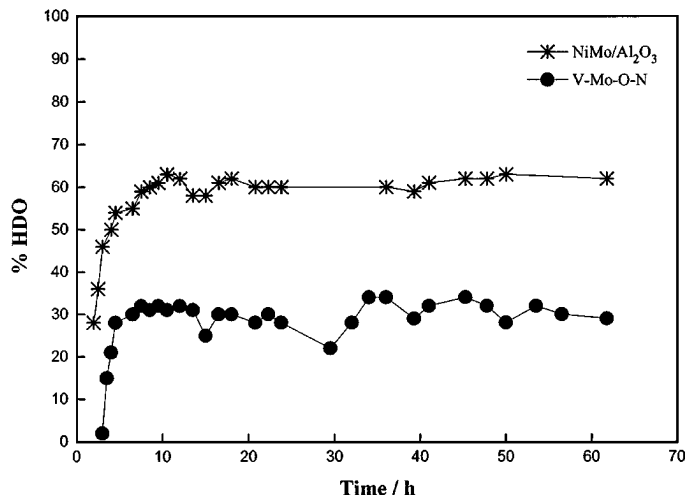


FIG. 3. Comparison of HDO activities of Ni-Mo/Al₂O₃ and V-Mo-O-N at 3.1 MPa and 643 K.

Figure 3 shows a comparison of the HDO activities of the most active catalysts. The Ni-Mo/Al₂O₃ catalyst showed higher HDO activity than the bimetallic oxynitrides. The major hydrocarbon products from HDO of benzofuran were ethylcyclohexane and ethylbenzene. Interestingly, among the monometallic compounds of Groups 4–6, VN showed the highest activity for HDO (12). This may be associated with an optimal binding energy for oxygen by the vanadium component.

The total activity (HDN, HDS, HDO, and HYD) and the HDN activity are reported in the form of turnover rates in Table 3 and as conversions at constant surface area loaded (30 m²) in Fig. 4. The turnover rates are based on CO chemisorption for the nitrides and O₂ chemisorption for the Ni-Mo-S/Al₂O₃. Measurement of CO uptakes is an accepted method for titrating surface metal atoms in the nitrides (12, 17). However as discussed earlier, the uptakes

TABLE 3

Comparison of the Turnover Rates of Bimetallic and Monometallic Nitrides at 3.1 MPa and 643 K

Catalyst	Total turnover rate (s ⁻¹) (HYD + HDN + HDS + HDO)	HDN turnover rate (s ⁻¹)
Ni-Mo/Al ₂ O ₃	2.0 × 10 ⁻³	4.5 × 10 ⁻⁴
V-Mo-O-N	2.9 × 10 ⁻³	1.0 × 10 ⁻³
Mo-W-O-N	1.1 × 10 ⁻²	3.6 × 10 ⁻³
Cr-Mo-O-N	2.8 × 10 ⁻³	9.1 × 10 ⁻⁴
Nb-Mo-O-N	5.8 × 10 ⁻²	1.6 × 10 ⁻²
Co-W-O-N	2.2 × 10 ⁻²	4.7 × 10 ⁻³
Co-Mo-O-N	3.0 × 10 ⁻³	6.5 × 10 ⁻⁴
Mn-Mo-O-N	1.6 × 10 ⁻²	3.7 × 10 ⁻³
V-W-O-N	1.9 × 10 ⁻²	3.1 × 10 ⁻⁴
Mo ₂ N	2.0 × 10 ⁻³	4.8 × 10 ⁻⁴
VN	4.5 × 10 ⁻³	2.6 × 10 ⁻⁴
TiN	1.2 × 10 ⁻³	7.6 × 10 ⁻⁵

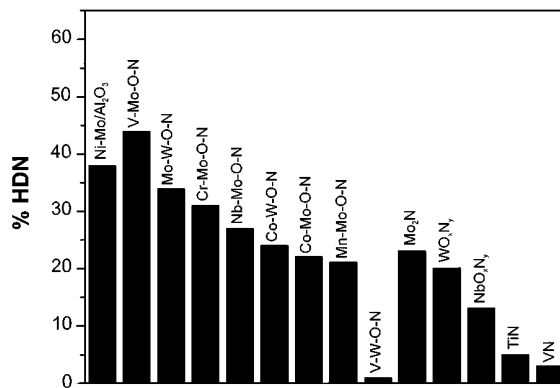


FIG. 4. Comparison of the %HDN conversion based on equal surface area loaded (30 m²) with bimetallic and monometallic oxynitrides at 3.1 MPa and 643 K.

on some of the materials may be low because of site blockage by surface N and O atoms. Chemisorption of O₂ for characterizing sulfides (18) is a more controversial method, but in the case of the Ni-Mo-S/Al₂O₃ used here, it gives a value that corresponds to about a monolayer of absorbed oxygen (5) consistent with the picture of a well dispersed catalyst. Overall, the results (Table 3, Fig. 4) indicate that the best bimetallic compounds are considerably more active than the monometallic catalysts and the commercial Ni-Mo/Al₂O₃ catalyst.

The catalytic reactivity reported in this paper is entirely due to the intrinsic activity of the catalysts and is not limited by internal or external mass transfer. A Thiele modulus calculation for the catalyst with the highest HDN conversion, V-Mo-O-N, was used to determine the lack of influence of internal diffusion. The observed reaction rate (1.1 × 10⁻⁸ mol (N removed) g⁻¹ s⁻¹ for V-Mo-O-N) and the effective diffusivity of quinoline in tetradecane (corrected for viscosity and density at 643 K (19)) were used to calculate the Thiele modulus using the equation (20)

$$\phi^2 = \frac{r_A \rho_p R^2}{D_{AB} C_A}$$

where r_A is the observed reaction rate (mol g⁻¹ s⁻¹), ρ_p is the catalyst packing density (g cm⁻³), R is the catalyst particle size (cm), C_A is the concentration of the reactant (mol cm⁻³), and D_{AB} is the effective diffusivity of the reactant (cm² s⁻¹). The effective diffusivity of quinoline in tetradecane was calculated using the equation applicable for dilute solutions (21),

$$D_{AB} = \frac{(117.3 \times 10^{-18})(\varphi M_B)^{0.5} T}{\mu V_A^{0.6}}$$

where D_{AB} is the diffusivity of A in very dilute solution in solvent B, M_B is the molecular weight of the solvent, T is the temperature, μ is the solution viscosity, V_A is the solute molal volume at normal boiling point, and φ is the

association factor for the solvent (1.0 for unassociated solvents). Based on the above equation, the effective diffusivity of quinoline in tetradecane at 643 K was calculated to be $1.5 \times 10^{-9} \text{ cm}^2 \text{ s}^{-1}$. The catalysts used in all the reactions were of $1 \mu\text{m}$ particle size, and the packing density was assumed to be 2 g cm^{-3} . The calculated value of ϕ was found to be 0.04, indicating negligible influence of internal diffusion on the observed rate. The influence of external mass transfer was calculated using the equation (22)

$$r_A = \frac{P_b}{(1/k_A) + (1/k)},$$

where r_A is the observed reaction rate, P_b is the bulk partial pressure, k_A is the mass transfer rate constant, and k is the reaction rate constant. In the above equation, if k is much greater than k_A , then external mass transfer would be the rate controlling step. k_A was calculated using the equation

$$k_A = \left(\frac{0.57 a_v \Phi}{\rho_b} \right) \left(\frac{G}{P_b M_m} \right) (N_{Re})^{-0.41} (N_{Sc})^{-2/3},$$

where a_v is the interfacial area for mass transfer per unit volume of the empty reactor bed ($6 \times 10^4 \text{ cm}^2$); ρ_b is the bulk density of the catalyst bed (2 g cm^{-3}), Φ is the shape factor (1 for spheres), G is the mass flow rate per unit of cross-sectional area ($6.15 \text{ g cm}^{-2} \text{ s}^{-1}$), M_m is the molecular weight of the mixture (198.9 g mol^{-1}), N_{Re} is the Reynolds number ($G/a_v \Phi \mu$); and N_{Sc} is the Schmidt number ($\mu/\rho D_{AB}$), where μ is the solution viscosity.

The value of k_A was calculated to be $1.8 \times 10^{-9} \text{ mol cm}^{-3} \text{ Pa}^{-1} \text{ s}^{-1}$, while the value of k was calculated to be $7.1 \times 10^{-15} \text{ mol cm}^{-3} \text{ Pa}^{-1} \text{ s}^{-1}$ (based on the observed reaction rate of $2.2 \times 10^{-8} \text{ mol of } N \text{ removed/cm}^3 \text{ s}$) for the V-Mo-O-N catalyst at 643 K and 3.1 MPa. Comparison of

the mass transfer and the reaction rate constants indicates that the activity values reported earlier were not influenced by external mass transfer. The reactions were carried out under bubble bed conditions which are standard for industrial conditions (5). The above calculations indicate that the observed reaction rates were limited neither by the diffusion of the reactant from the liquid phase to the catalyst surface nor by intraparticle diffusion.

Quinoline Hydrodenitrogenation Network

Figure 5 presents the proposed reaction network for quinoline HDN based on the products identified using a gas chromatograph. Products detected from quinoline HDN were partially hydrogenated quinoline compounds of 1,2,3,4 tetrahydroquinoline and 5,6,7,8 tetrahydroquinoline and hydrodenitrogenated hydrocarbons like propylcyclohexane and propylbenzene. *o*-Propylaniline (OPA) was also detected in small amounts. Decahydroquinoline (DHQ) was not detected in the products from any of the reactions, indicating that this compound was highly reactive at the reaction conditions, but the possibility of fast hydrogenation to propylcyclohexylamine (PCHA) and further deamination to hydrocarbons cannot be ruled out. To get a better understanding of the reaction network, 0.2 wt% of OPA (steady state concentration = 5.4 mol%) and 0.2 wt% of DHQ were added to the regular feed mixture and the reaction was carried out using the V-Mo-O-N catalyst. The results of this reaction indicated that OPA was unreactive under the reaction conditions, while DHQ was completely converted to hydrocarbons. In fact, DHQ reacted completely to hydrocarbons even at 523 K. Similarly, results from the addition of 0.2 wt% of 1-THQ (steady state concentration = 20 mol%) and 0.2 wt% of 5-THQ (steady state concentration = 18 mol%) to the regular feed mixture

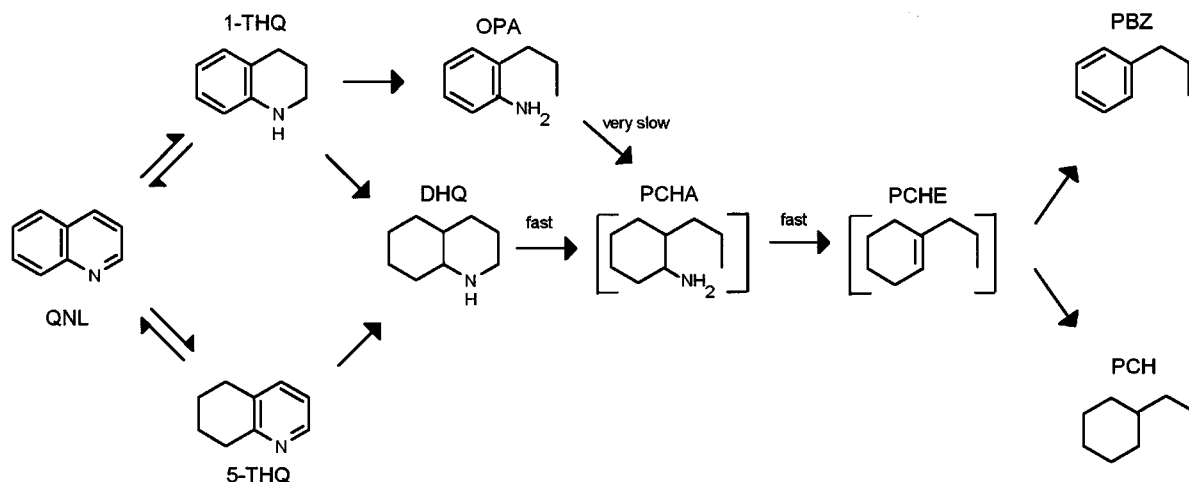


FIG. 5. Proposed quinoline HDN reaction network. QNL denotes quinoline; 1-THQ, 1,2,3,4 tetrahydroquinoline; 5-THQ, 5,6,7,8 tetrahydroquinoline; DHQ, decahydroquinoline; OPA, *o*-propylaniline; PCHA, propylcyclohexylamine; PCHE, propylcyclohexene; PCH, propylcyclohexane; and PBZ, propylbenzene.

indicated that the rate of hydrogenation of 1-THQ to DHQ was comparable to that of 5-THQ to DHQ. Clearly, quinoline HDN over V-Mo-O-N seems to proceed through a reaction pathway involving saturation of both aromatic rings in quinoline and a rapid hydrogenolysis of DHQ to yield hydrocarbons. The rate limiting step appears to be the hydrogenation of OPA to propylcyclohexylamine. Satterfield and Yang (23) proposed a reaction network for gas-phase quinoline HDN over sulfided Ni-Mo/Al₂O₃ catalyst involving the hydrogenation of both aromatic rings of quinoline and a subsequent hydrogenolysis of DHQ to hydrocarbons. However, they suggested that most of the denitrogenation occurred via 5-THQ as intermediate.

The presence of oxygen in the metal lattice should have improved the acidity of the catalysts and in turn the isomerization activity. However, there were no isomerized products detected and this could be due to the replacement of oxygen by sulfur on the surface of the catalysts which suppressed the isomerization activity.

Catalyst Characterization

Figure 6 presents the X-ray diffraction patterns of the spent catalysts. Extraneous sulfide or oxide peaks were not observed in the XRD patterns of the compounds involving Groups 4–6 metals, indicating that these catalysts

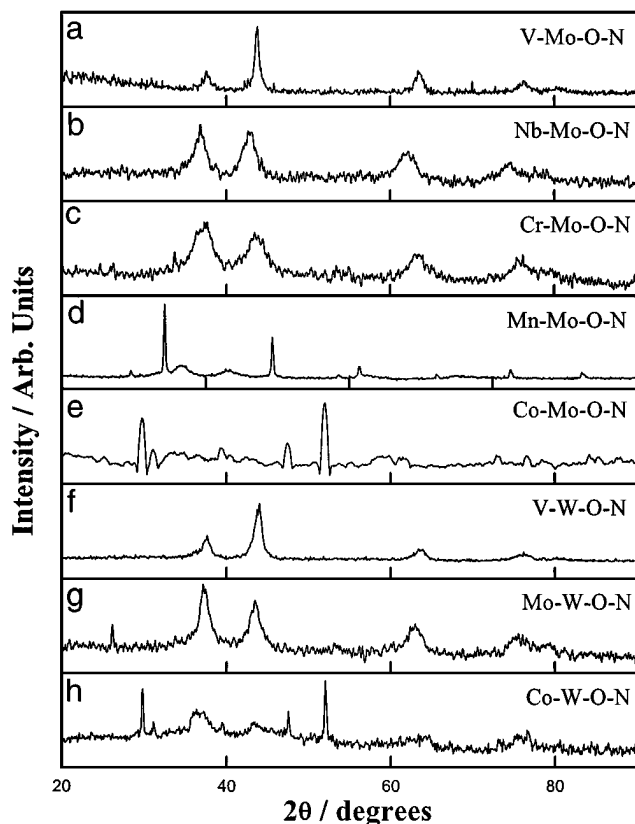


FIG. 6. X-ray diffraction patterns of the spent catalysts.

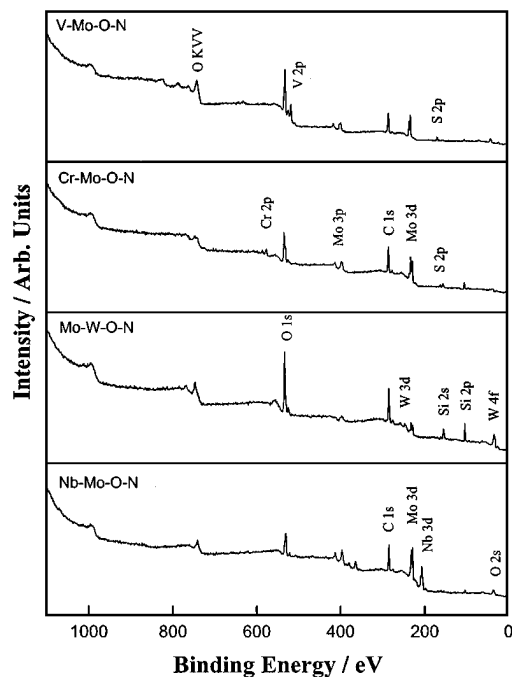


FIG. 7. X-ray photoelectron spectroscopic analysis of the sulfur composition of the spent catalysts.

were stable toward sulfur and oxygen at the reaction conditions. However, compounds involving Mn and Co as one of the elements showed sulfide phases in the bulk. Spent Mn-Mo-O-N showed sharp peaks of MnS as seen in Fig. 6. The broad peaks of the fresh sample can still be identified apart from the MnS features, indicating that the initial structure was still preserved, except that some of the manganese in the bulk was converted into MnS. In the case of Co-containing compounds, the spent catalysts showed sharp features of Co₄S₃. Co-W-O-N had some features of the initial pattern apart from Co₄S₃ peaks, while Co-Mo-O-N did not retain any features of the fresh sample. This is probably due to the better sulfur tolerance over molybdenum which resulted in only Co being converted to Co₄S₃ in Co-W-O-N.

XPS analysis was carried out to look for changes in the surface composition of the catalysts after the reaction. Figure 7 presents the XPS spectra obtained for the sulfur tolerant catalysts after the reaction. The results presented in Table 4 show the presence of excess graphitic carbon (285.0 eV) and oxygen (531.4 eV) as metal oxides on the surface of the fresh catalysts. These were due to exposure of the materials to the atmosphere, as *in situ* reduction was not carried out prior to the XPS analysis. The unusually low N/Metal ratio in fresh V-Mo-O-N and Co-Mo-O-N could be due to the deposition of more than one atomic layer of oxide on the surface during passivation. The XPS spectra (Fig. 7) and the S/Metal ratio (Table 4) indicate that there was moderate sulfur incorporation on the surface of

TABLE 4
Atomic Concentration Ratios of Nonmetal
to Metal Analyzed by XPS

Fresh catalyst	C/Metal ^a	O/Metal ^a	N/Metal ^a	S/Metal ^a
V-Mo-O-N	2.22	2.33	0.09	0.00
Nb-Mo-O-N	1.62	1.42	0.86	0.00
Cr-Mo-O-N	2.71	2.42	1.00	0.00
Mo-W-O-N	2.62	1.72	0.83	0.00
Spent catalyst	C/Metal ^a	O/Metal ^a	N/Metal ^a	S/Metal ^a
V-Mo-O-N	2.93	1.19	0.14	0.25
Nb-Mo-O-N	2.96	1.71	0.75	0.19
Cr-Mo-O-N	4.60	3.00	1.10	0.30
Mo-W-O-N	8.59	6.05	0.63	0.15

^a Metal = combined concentration of M_I and M_{II} .

the spent catalysts. Interestingly, a sulfide phase (161.9 eV) was identified in all the catalysts, except V-Mo-O-N, which showed predominantly a sulfate phase (169.1 eV) (13). The maximum sulfur concentration was detected for Co-Mo and Co-W consistent with the XRD analysis, while bimetallic compounds consisting of metals from Groups 4-6 with W as one of the metals seemed to be more resistant to sulfur incorporation. In all cases higher sulfur levels were observed with a lower initial nitrogen level, indicating that nitrogen played a role in stabilizing the surface composition. It is likely that in cases where nitrogen levels were low, sulfur exchanged with oxygen. The sulfate phase observed with the V-Mo-O-N could be the result of oxidation of a chemisorbed sulfur layer at the surface. In contrast to the other samples in which a sulfide phase was detected, the lack of a sulfide layer in this case could be associated with the high catalytic activity of the material for HDN.

CONCLUSIONS

The bimetallic oxynitrides were found to possess excellent HDN activity and, in particular, V-Mo-O-N showed better HDN activity than the commercial sulfided Ni-Mo/Al₂O₃ catalyst. Bimetallic oxynitrides with molybdenum as one of the metals showed higher activity than the corresponding monometallic nitrides. Molybdenum or tungsten alloyed with early transition metals (V, Nb, Cr) were sulfur tolerant, while Mn and Co alloys were

sulfur sensitive and showed bulk sulfidation. The activity results are promising and further work needs to be carried out to optimize the ratio of the concentration of metals in the bimetallic compounds.

ACKNOWLEDGMENTS

This work was carried out with support from the Department of Energy, Office of Basic Energy Sciences, Grant DE-FG02-96ER14669, the D.O.E. Advanced Coal Research at U.S. Universities Program, Grant DE-FG26-97FT97265, and Akzo Nobel. We thank B. Dhandapani, T. St. Clair, and V. L. S. Teixeira da Silva for their assistance in the activity measurements.

REFERENCES

- Katzer, J. R., and Sivasubramaniam, R., *Catal. Rev.-Sci. Eng.* **20**, 155 (1979).
- Ho, T. C., *Catal. Rev.-Sci. Eng.* **30**(1), 117 (1988).
- Oyama, S. T., *Catal. Today* **15**, 179 (1992).
- Schlatter, J. C., Oyama, S. T., Metcalfe, J. E., III., and Lambert, J. M., Jr., *Ind. Eng. Chem. Res.* **27**, 1648 (1988).
- Sajkowski, D. J., and Oyama, S. T., *Appl. Catal. A* **134**, 339 (1996).
- Lee, K. S., Abe, H., Reimer, J. A., and Bell, A. T., *J. Catal.* **139**, 34 (1993).
- Colling, W. C., and Thompson, L. T., *J. Catal.* **146**, 193 (1994).
- Abe, H., and Bell, A. T., *Catal. Lett.* **18**, 1 (1993).
- Nagai, M., and Miyao, T., *Catal. Lett.* **15**, 105 (1992).
- Markel, E. J., and Van Zee, J. W., *J. Catal.* **126**, 643 (1990).
- Abe, H., Cheung, T. K., and Bell, A. T., *Catal. Lett.* **21**, 11 (1993).
- Ramanathan, S., and Oyama, S. T., *J. Phys. Chem.* **99**, 16365 (1995).
- Moulder, J. F., Stickle, W. F., Sobol, P. E., and Bomben, K. D., in "Handbook of X-ray Photoelectron Spectroscopy" (J. Chastain, Ed.), Perkin Elmer, Physical Electronics Division, 1992.
- Yu, C. C., Ramanathan, S., Sherif, F., and Oyama, S. T., *J. Phys. Chem.* **98**, 13038 (1994).
- Pecoraro, T. A., and Chianelli, R. R., *J. Catal.* **67**, 430 (1981).
- Harris, S., and Chianelli, R. R., *J. Catal.* **86**, 400 (1984).
- Lee, J. S., Lee, K. H., and Lee, J. Y., *J. Phys. Chem.* **96**, 362 (1992).
- Tauster, S. J., Pecoraro, T. A., and Chianelli, R. R., *J. Catal.* **63**, 515 (1980).
- Reid, R. C., Prausnitz, J. M., and Sherwood, T. K., "The Properties of Gases and Liquids," 3rd ed., McGraw-Hill, New York, 1977.
- Fogler, S. H., "Elements of Chemical Reaction Engineering," 2nd ed., Prentice-Hall, Englewood Cliffs, NJ, 1992.
- Treybal, R. E., in "Mass Transfer Operations," 3rd ed., McGraw-Hill, New York, 1981.
- Holland, C. D., and Anthony, R. G., "Fundamentals of Chemical Reaction Engineering," 2nd ed., Prentice-Hall, Englewood Cliffs, NJ, 1989.
- Satterfield, C. N., and Yang, S. H., *Ind. Eng. Chem. Proc. Des. Dev.* **23**, 11 (1984).
- Lucy, T., St. Clair, T., and Oyama, S. T., *J. Mater. Res.*, in press.
- Schwartz, V., and Oyama, S. T., *Chem. Mater.*, in press.